

Synthesis, Photophysics, and Optical Limiting of Platinum(II) 4'-Tolylterpyridyl Arylacetylide Complexes

Fengqi Guo and Wenfang Sun*

Department of Chemistry and Molecular Biology, North Dakota State University,
Fargo, North Dakota 58105-5516

Yao Liu and Kirk Schanze

Department of Chemistry, University of Florida, P.O. Box 117200,
Gainesville, Florida 32611-7200

Received June 5, 2004

A series of 4'-tolylterpyridyl platinum(II) complexes with different arylacetylide ligands, namely, phenylacetylide, 4-bromophenylacetylide, 4-nitrophenylacetylide, 4-methoxyphenylacetylide, 4-dimethylaminophenylacetylide, 1-naphthylacetylide, and 3-quinolinylacetylide, were synthesized. Their photophysical properties, such as electronic absorption spectra, emission characteristics at room temperature and 77 K, and transient difference absorption spectra, have been investigated. All of these complexes exhibit a metal-to-ligand charge-transfer (¹MLCT) transition at ca. 420–430 nm in their electronic absorption spectra. For ttpy-Ph, ttpy-C₆H₄Br-4, ttpy-C₆H₄OCH₃-4, ttpy-C₆H₄N(CH₃)₂-4, and ttpy-Np, an additional solvatochromic charge-transfer band appears at ca. 460–540 nm. This band is sensitive to the para substituents on the phenylacetylide ligand and is tentatively assigned to a metal- or/and acetylide-to-terpyridyl charge-transfer transition (i.e., a ¹MLCT or/and ¹LLCT transition). All of the complexes exhibit room-temperature phosphorescence. The emission can be attributed to a ³MLCT state except for ttpy-C₆H₄NO₂-4, for which the emission likely originates from an intraligand ³π,π* state involving the nitrophenylacetylide ligand. For ttpy-C₆H₄OCH₃-4, ttpy-C₆H₄N(CH₃)₂-4, and ttpy-Np, there probably is more than one low-energy state in close energy proximity, resulting in multiple exponential decays. In addition, the triplet transient absorption difference spectra of ttpy-Ph, ttpy-C₆H₄Br-4, ttpy-C₆H₄NO₂-4, and ttpy-Quin exhibit moderately intense, broad absorption bands in the visible region and extending into the near-IR region, which likely originate from the same excited state that emits or from a state that is in equilibrium with the emitting state. It appears that the electron-rich arylacetylide ligands, especially 4-methoxyphenylacetylide and 4-dimethylaminophenylacetylide, cause a decrease of the emission efficiency and disappearance of the transient absorption. In contrast, the complexes that exhibit positive absorption bands in the visible spectral region of the triplet transient difference absorption spectra show substantial optical limiting for nanosecond laser pulses at 532 nm.

Introduction

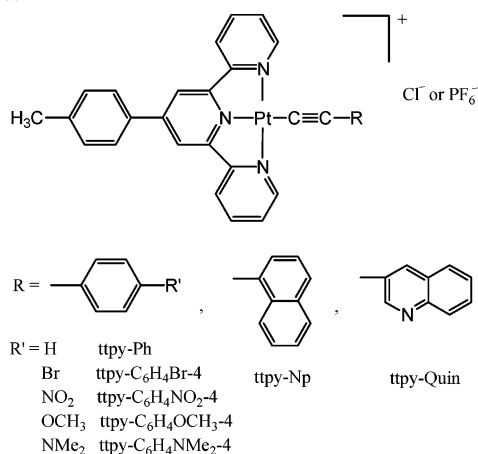
Square-planar platinum(II) terpyridyl complexes have attracted great interest in recent years because of their unique spectroscopic properties^{1–8} and their potential applications

as DNA intercalators^{9,10} and protein probes.¹¹ Recently, platinum(II) terpyridyl phenylacetylide complexes were

* To whom correspondence should be addressed. Tel.: 701-231-6254. Fax: 701-231-8831. E-mail: Wenfang.Sun@ndsu.nodak.edu.

- (1) Aldridge, T. K.; Stacey, E. M.; McMillin, D. R. *Inorg. Chem.* **1994**, *33*, 722.
- (2) Büchner, R.; Field, J. S.; Haines, R. J.; Cunningham, C. T.; McMillin, D. R. *Inorg. Chem.* **1997**, *36*, 3952.
- (3) Crites, D. K.; Cunningham, C. T.; McMillin, D. R. *Inorg. Chim. Acta* **1998**, *273*, 346.

- (4) Büchner, R.; Cunningham, C. T.; Field, J. S.; Haines, R. J.; McMillin, D. R.; Summerton, G. C. *J. Chem. Soc., Dalton Trans.* **1999**, 711.
- (5) Lai, S.-W.; Chan, M. C. W.; Cheung, K.-K.; Che, C.-M. *Inorg. Chem.* **1999**, *38*, 4262.
- (6) Yam, V. W.-W.; Tang, R. P.-L.; Wong, K. M.-C.; Cheung, K.-K. *Organometallics* **2001**, *20*, 4476.
- (7) Michalec, J. F.; Bejune, S. A.; Cuttall, D. G.; Summerton, G. C.; Gertenbach, J. A.; Field, J. S.; Haines, R. J.; McMillin, D. R. *Inorg. Chem.* **2001**, *40*, 2193.
- (8) Yang, Q.-Z.; Wu, L.-Z.; Wu, Z.-X.; Zhang, L.-P.; Tung, C.-H. *Inorg. Chem.* **2002**, *41*, 5653.

Chart 1. Chemical Structures of 4'-Tolylterpyridyl Arylacetylide Complexes

demonstrated by our group¹² to exhibit strong reverse saturable absorption (RSA) for nanosecond laser pulses, suggesting that this class of complexes represents promising broadband optical limiting materials. These results are intriguing; however, our previous study focused only on the effect of conjugation length of the phenylacetylide ligand and the possible influence of the 4'-substituent on the 4-phenyl ring of the terpyridyl ligand. The effect of different aryl substituents on the acetylide ligand on the RSA and the photophysics of the complexes has not been evaluated. It has been demonstrated that the nature of the acetylide ligand has a significant effect on the emission properties of platinum complexes.^{3,6-8} Therefore, it is expected that different arylacetylide ligands will have a significant effect on their excited-state absorption and, in turn, on their optical limiting properties. To demonstrate this, a series of platinum 4'-tolylterpyridyl arylacetylide complexes (Chart 1) has been synthesized and characterized. The effects of the arylacetylide ligands on the ground-state and excited-state energy levels and lifetimes and triplet excited-state transient difference absorption spectra have been systematically investigated. The optical limiting performances of several complexes have also been explored using 4.1-ns laser pulses at 532 nm. From these studies, we intend to better understand the correlation between the electronic characteristics of the arylacetylide ligand and the photophysical properties in order to develop new platinum(II) terpyridyl arylacetylide complexes with long-lived excited states and strong excited-state absorption for application in optical power limiting.

Experimental Section

Synthesis. The platinum 4'-tolylterpyridyl arylacetylide complexes were synthesized by modification of literature procedures.^{5,6,13} 4'-(4-Methylphenyl)-2,2':6',2''-terpyridine (ttpy) and 1-

bromo-4-ethynylbenzene were purchased from Aldrich Chemical Co. Potassium tetrachloroplatinate and *trans*-dichlorobis(triphenylphosphine)palladium(II) were obtained from Alfa Aesar. Phenylacetylene, 1-bromo-4-nitrobenzene, 4-bromoanisole, 4-bromo-*N,N*-dimethylaniline, 1-iodonaphthalene, 3-bromoquinoline, and trimethylsilylacetylene were obtained from Avocado Research Chemical Ltd. All solvents purchased from VWR Scientific Products were analytical grade and were used directly without further purifications. *p*-Nitroethynylbenzene, *p*-ethynylanisole, *p*-(dimethylamino)phenylacetylene, 1-ethynyl-naphthalene, and 3-ethynylquinoline were synthesized according to literature procedures.^{14,15}

The synthesized compounds were characterized by UV-vis, IR, NMR, ESI-HRMS, and elemental analyses. UV-vis spectra were obtained using a CARY 500 dual-beam scanning UV-vis-NIR spectrophotometer. IR spectra were measured on a Thermo Nicolet Fourier transform infrared spectrophotometer. ¹H NMR and ¹³C NMR spectra were measured on an Oxford 300 MHz VNMR spectrometer. Electrospray ionization (ESI) high-resolution mass spectrometry analyses were conducted on a 3-Tesla Finnigan FTMS-2000 Fourier transform mass spectrometer. Elemental analyses were performed on a Perkin-Elmer 2400 Series II CHNS/O analyzer.

***p*-Ethynylanisole.** *p*-Ethynylanisole was synthesized according to the literature procedure.¹⁴ Yield: 61%. ¹H NMR (CDCl₃) δ: 3.01 (s, 1H), 3.80 (s, 3H), 6.90 (d, 2H, *J* = 8.5 Hz), 7.50 (d, 2H, *J* = 8.5 Hz) ppm. ¹³C NMR (CDCl₃) δ: 55.5, 76.1, 84.0, 115.0, 129.0, 134.0, 134.7, 160.5 ppm.

1-Ethynyl-naphthalene. 1-Ethynyl-naphthalene was synthesized by modification of the literature procedure.¹⁴ 1-Iodonaphthalene (1.28 g, 5 mmol) and trimethylsilylacetylene (0.99 g, 10 mmol) were dissolved in 20 mL of triethylamine. Bis(triphenylphosphine) palladium dichloride (70 mg, 0.1 mmol) and CuI (5 mg, 0.026 mmol) were added to this mixture. The reaction mixture was stirred at room temperature for 16 h, and then the mixture was heated to reflux for 2 h. After being allowed to cool, the solvent was removed under reduced pressure. A 15 mL portion of methanol was added to dissolve the residue, and 1 N aqueous potassium hydroxide solution (5 mL) was added. The mixture was stirred at room temperature for 2 h. Methanol was removed, and the aqueous solution was extracted with ether (3 × 50 mL). The ether layer was dried over MgSO₄, and then the solvent was removed. The crude product was purified using column chromatography (silica gel 60 mesh), with a 1:1 benzene/hexane mixture used as the eluent. Yield: 27%. ¹H NMR (CDCl₃) δ: 3.55 (s, 1H), 7.48 (t, 1H, *J* = 8.3 Hz), 7.62 (m, 2H), 7.82 (d, 1H, *J* = 6.7 Hz), 7.90 (d, 2H, *J* = 8.3 Hz), 8.47 (d, 1H, *J* = 8.3 Hz) ppm. ¹³C NMR (CDCl₃) δ: 82.2, 82.5, 120.0, 125.5, 126.5, 127.0, 127.5, 128.8, 129.6, 131.9, 133.5, 133.8 ppm.

3-Ethynylquinoline. The procedure was similar to that for 1-ethynyl-naphthalene, except that 3-bromoquinoline was used to replace 1-iodonaphthalene. Yield: 27%. ¹H NMR (CDCl₃) δ: 3.20 (s, 1H), 7.59 (m, 1H), 7.68 (m, 2H), 8.10 (d, 1H, *J* = 7.2 Hz), 8.25 (s, 1H), 8.95 (s, 1H) ppm. ¹³C NMR (CDCl₃) δ: 80.8, 81.2, 101.0, 116.5, 127.5, 127.7, 129.8, 130.8, 139.7, 147.5, 152.1 ppm.

[Pt(ttpy)Cl]Cl. [Pt(ttpy)Cl]Cl was synthesized by a slight modification of the literature procedure.⁵ After being refluxed for 24 h in acetonitrile/water, the yellow solid was separated by filtration, dried under reduced pressure, and recrystallized in ethanol.

(9) Lippard, S. J. *Acc. Chem. Res.* **1978**, *11*, 211.

(10) Arena, G.; Monsú Scolaro, L.; Pasternack, R. F.; Romeo, R. *Inorg. Chem.* **1995**, *34*, 2994.

(11) Ratilla, E. M. A.; Brothers, H. M., II.; Kostia, N. M. *J. Am. Chem. Soc.* **1987**, *109*, 4592.

(12) Sun, W.; Wu, Z.-X.; Yang, Q.-Z.; Wu, L.-Z.; Tung, C.-H. *Appl. Phys. Lett.* **2003**, *82*(6), 850.

(13) Hissler, M.; Connick, W. B.; Geiger, D. K.; McGarrah, J. E.; Lipa, D.; Lachicotte, R. J.; Eisenberg, R. *Inorg. Chem.* **2000**, *39*, 447.

(14) Takahashi, S.; Kuroyama, Y.; Sonogashira, K.; Hagihara, N. *Synthesis* **1980**, 627.

(15) Leonard, K. A.; Nelen, M. I.; Anderson, L. T.; Gibson, S. L.; Hilf, R.; Detty, M. R. *J. Med. Chem.* **1999**, *42*, 3942.

General Procedure for the Synthesis of [Pt(ttpy)(C≡CC₆H₄R)]-Cl (**R** = **Br**, **N(CH₃)₂**, **OCH₃**, **NO₂**). The procedure was modified from literature procedures.^{6,8} Potassium hydroxide (20 mg, 0.36 mmol) was added to 50 mL of a methanol solution of arylacetylene (0.24 mmol), and the mixture was stirred at room temperature for 30 min. [Pt(ttpy)Cl]Cl (120 mg, 0.2 mmol) and CuI (5 mg, 0.026 mmol) were added to the reaction mixture, and the resultant solution was stirred at room temperature for 12 h. During the reaction, solid gradually precipitated. The precipitate was isolated by filtration and recrystallized from DMF and ether.

[Pt(ttpy)(C≡CC₆H₄Br)]Cl. Yield: 68%. ¹H NMR (DMSO-*d*₆) δ: 2.48 (s, 3H), 7.15 (d, 2H, *J* = 4.5 Hz), 7.33 (m, 4H), 7.61 (m, 2H), 7.87 (d, 2H, *J* = 5 Hz), 8.30 (t, 2H), 8.59 (m, 4H), 8.75 (m, 2H) ppm. IR (KBr) *ν*: 2110 [w, *ν*(C≡C)] cm⁻¹. ESI-MS: *m/z* calcd for [C₃₀H₂₁BrN₃Pt¹⁹⁴]⁺ 697.0902, found 697.0523 (58%); calcd for [C₃₀H₂₁BrN₃Pt¹⁹⁵]⁺ 698.0923, found 698.0467 (100%); calcd for [C₃₀H₂₁BrN₃Pt¹⁹⁶]⁺ 699.0925, found 699.0469 (72%). Anal. Calcd for C₃₀H₂₁BrClN₃Pt·3H₂O: C, 45.60; H, 3.43; N, 5.46. Found: C, 45.97; H, 3.53; N, 5.65.

[Pt(ttpy)(C≡CC₆H₄N(CH₃)₂)]Cl. Yield: 67%. ¹H NMR (DMSO-*d*₆) δ: 2.45 (s, 3H), 2.90 (s, 6H), 6.60 (d, 2H, *J* = 8.7 Hz), 7.15 (d, 2H, *J* = 8.7 Hz), 7.45 (d, 2H, *J* = 8.7 Hz), 7.75 (t, 2H, *J* = 9.0 Hz), 8.00 (d, 2H, *J* = 8.7 Hz), 8.40 (t, 2H, *J* = 9.0 Hz), 8.72 (d, 2H, *J* = 8.7 Hz), 8.80–9.00 (m, 4H) ppm. IR (KBr) *ν*: 2110 [w, *ν*(C≡C)] cm⁻¹. ESI-MS: *m/z* calcd for [C₃₂H₂₇N₄Pt¹⁹⁴]⁺ 661.2623, found 661.1880 (72%); calcd for [C₃₂H₂₇N₄Pt¹⁹⁵]⁺ 662.2644, found 662.1885 (100%); calcd for [C₃₂H₂₇N₄Pt¹⁹⁶]⁺ 663.2646, found 663.1871 (92%). Anal. Calcd for C₃₂H₂₇N₄PtCl·3H₂O: C, 51.06; H, 4.35; N, 5.58. Found: C, 50.66; H, 3.62; N, 5.60.

[Pt(ttpy)(C≡CC₆H₄OCH₃)]Cl. Yield: 64%. ¹H NMR (DMSO-*d*₆) δ: 2.41 (s, 3H), 3.75 (s, 3H), 6.85 (d, 2H, *J* = 9.0 Hz), 7.33 (d, 2H, *J* = 9.0 Hz), 7.43 (d, 2H, *J* = 9.0 Hz), 7.79 (t, 2H), 8.05 (d, 2H), 8.40 (m, 2H), 8.75 (m, 2H), 8.90 (m, 4H) ppm. IR (KBr) *ν*: 2110 [w, *ν*(C≡C)] cm⁻¹. ESI-MS: *m/z* calcd for [C₃₁H₂₄N₃OPt¹⁹⁴]⁺ 648.2203, found 648.1500 (74%); calcd for [C₃₁H₂₄N₃OPt¹⁹⁵]⁺ 649.2224, found 649.1571 (100%); calcd for [C₃₁H₂₄N₃OPt¹⁹⁶]⁺ 650.2226, found 650.1569 (74%). Anal. Calcd for C₃₁H₂₄N₃OClPt·3H₂O: C, 50.38; H, 4.06; N, 5.60. Found: C, 50.70; H, 3.60; N, 5.46.

[Pt(ttpy)(C≡CC₆H₄NO₂)]Cl. Yield: 31%. ¹H NMR (DMSO-*d*₆) δ: 2.46 (s, 3H), 7.33 (d, 2H, *J* = 8.2 Hz), 7.47 (d, 2H, *J* = 8.2 Hz), 7.66 (t, 2H, *J* = 6.8 Hz), 7.95 (t, 4H, *J* = 8.2 Hz), 8.40 (t, 2H, *J* = 8.2 Hz), 8.60–8.90 (m, 6H) ppm. IR (KBr) *ν*: 2110 [w, *ν*(C≡C)] cm⁻¹. ESI-MS: *m/z* calcd for [C₃₀H₂₁N₄O₂Pt¹⁹⁴]⁺ 663.1917, found 663.1180 (71%); calcd for [C₃₀H₂₁N₄O₂Pt¹⁹⁵]⁺ 664.1938, found 664.1273 (100%); calcd for [C₃₀H₂₁N₄O₂Pt¹⁹⁶]⁺ 665.1940, found 665.1392 (79%). Anal. Calcd for C₃₀H₂₁N₄O₂ClPt·5H₂O: C, 45.50; H, 3.90; N, 7.01. Found: C, 45.14; H, 3.33; N, 7.06.

[Pt(ttpy)(C≡CC₆H₅)]Cl. The synthesis of [Pt(ttpy)(CCC₆H₅)]-Cl followed the general procedure described above, except for the following: After 12 h of reaction at room temperature, the mixture was filtered, and 100 mL of ether was added to the filtrate, yielding the crude product. The crude product was isolated and recrystallized from methanol and ether. Dark purple powder was collected (yield: 57%). ¹H NMR (CD₃OD) δ: 2.42 (s, 3H), 6.91 (d, 2H, *J* = 6.6 Hz), 7.10 (m, 3H), 7.30 (m, 4H), 7.55 (d, 2H, *J* = 9.3 Hz), 8.00 (t, 2H), 8.09 (d, 2H, *J* = 9.3 Hz), 8.20 (2H), 8.25 (d, 2H, *J* = 6.3 Hz) ppm. IR (KBr) *ν*: 2150 [w, *ν*(C≡C)] cm⁻¹. ESI-MS: *m/z* calcd for [C₃₀H₂₂N₃Pt¹⁹⁴]⁺ 618.1941, found 618.1515 (68%); calcd for [C₃₀H₂₂N₃Pt¹⁹⁵]⁺ 619.1962, found 619.1453 (100%); calcd for [C₃₀H₂₂N₃Pt¹⁹⁶]⁺ 620.1964, found 620.1426 (84%). Anal. Calcd for C₃₀H₂₂ClN₃Pt·2H₂O: C, 52.10; H, 3.70; N, 6.06. Found: C, 51.90; H, 3.84; N, 6.07.

General Procedure for the Synthesis of [Pt(ttpy)(C≡CC₆H₄R)]-PF₆. The synthesized [Pt(ttpy)(C≡CC₆H₄R)]Cl complexes (0.2 mmol) were dissolved in 20 mL of DMF, and 65 mg of NH₄PF₆ (0.4 mmol) and 40 mL of CH₃OH were added. After the mixture had been stirred for 2 h at room temperature, the solids were separated by filtration and recrystallized from acetonitrile and ether.

[Pt(ttpy)(C≡CC₆H₅)]PF₆ (ttpy-Ph). Yield: 76%. ¹H NMR (CD₃CN) δ: 2.49 (s, 3H), 7.12–7.28 (m, 5H), 7.36–7.48 (m, 4H), 7.63 (d, 2H, *J* = 8.1 Hz), 8.00–8.20 (m, 6H), 8.55 (m, 2H) ppm. Anal. Calcd for C₃₀H₂₂N₃PtPF₆·H₂O: C, 46.03; H, 3.06; N, 5.37. Found: C, 46.34; H, 2.93; N, 5.47.

[Pt(ttpy)(C≡CC₆H₄Br)]PF₆ (ttpy-C₆H₄Br-4). Yield: 60%. ¹H NMR (CD₃CN) δ: 2.51 (s, 3H), 7.09 (d, 2H, *J* = 7.5 Hz), 7.30 (d, 2H, *J* = 7.5 Hz), 7.40 (m, 4H), 7.60 (d, 2H, *J* = 7.2 Hz), 8.10–8.24 (m, 6H), 8.58 (2H) ppm. Anal. Calcd for C₃₀H₂₁N₃BrPtPF₆·H₂O: C, 41.60; H, 2.67; N, 4.87. Found: C, 41.27; H, 2.50; N, 4.87.

[Pt(ttpy)(C≡CC₆H₄NO₂)]PF₆ (ttpy-C₆H₄NO₂-4). Yield: 55%. ¹H NMR (CD₃CN) δ: 2.40, 7.39, 7.50, 7.71, 8.00, 8.45, 8.82, 8.90 ppm. Anal. Calcd for C₃₀H₂₁N₄O₂PtPF₆·H₂O: C, 43.60; H, 2.66; N, 6.77. Found: C, 43.26; H, 2.52; N, 6.78.

[Pt(ttpy)(C≡CC₆H₄OCH₃)]PF₆ (ttpy-C₆H₄OCH₃-4). Yield: 72%. ¹H NMR (CD₃CN) δ: 2.49 (s, 3H), 3.75 (s, 3H), 6.60 (d, 2H, *J* = 6.3 Hz), 6.90 (d, 2H, *J* = 6.3 Hz), 7.30–7.40 (m, 4H), 7.50 (d, 2H, *J* = 5.7 Hz), 7.90–8.20 (m, 6H), 8.34 (m, 2H) ppm. Anal. Calcd for C₃₁H₂₄N₃OPtPF₆·H₂O: C, 45.87; H, 3.22; N, 5.17. Found: C, 45.69; H, 3.09; N, 5.28.

[Pt(ttpy)(C≡CC₆H₄N(CH₃)₂)]PF₆ (ttpy-C₆H₄N(CH₃)₂-4). Yield: 45%. ¹H NMR (CD₃CN) δ: 2.49 (s, 3H), 2.95 (s, 6H), 6.54 (d, 2H, *J* = 8.4 Hz), 7.06 (d, 2H, *J* = 7.2 Hz), 7.40 (d, 2H, *J* = 6.6 Hz), 7.49 (m, 2H), 7.70 (d, 2H, *J* = 6.9 Hz), 8.10–8.24 (m, 6H), 8.69 (m, 2H) ppm. Anal. Calcd for C₃₂H₂₇N₄PtPF₆: C, 47.54; H, 3.34; N, 6.93. Found: C, 47.19; H, 3.39; N, 6.91.

[Pt(ttpy)(C≡CC₁₀H₇)]PF₆ (ttpy-Np). The synthesis was similar to the general procedure for the synthesis of [Pt(ttpy)(C≡CC₆H₄R)]-Cl, except that 1-ethynyl naphthalene was used. After being stirred for 12 h at room temperature, the mixture was filtered, and a saturated solution of ammonium hexafluorophosphate in methanol was added to the filtrate. The product was isolated and recrystallized from acetonitrile and ether. Deep red product was obtained. Yield: 70%. ¹H NMR (CD₃CN) δ: 2.47 (s, 3H), 7.30–7.50 (m, 4H), 7.52–7.70 (m, 7H), 7.76–7.96 (m, 2H), 8.20–8.40 (m, 6H), 9.04 (m, 2H) ppm. IR (KBr) *ν*: 2110 [w, *ν*(C≡C)] cm⁻¹. ESI-MS: *m/z* calcd for [C₃₄H₂₄N₃Pt¹⁹⁴]⁺ 668.2539, found 668.1463 (76%); calcd for [C₃₄H₂₄N₃Pt¹⁹⁵]⁺ 669.2560, found 669.1563 (100%); calcd for [C₃₄H₂₄N₃Pt¹⁹⁶]⁺ 670.2562, found 670.1628 (99.9%). Anal. Calcd for C₃₄H₂₄N₃PtPF₆: C, 50.0; H, 2.97; N, 5.15. Found: C, 49.70; H, 3.03; N, 4.92.

[Pt(ttpy)(C≡CC₉H₆N)]PF₆ (ttpy-Quin). The procedure was similar to that for complex [Pt(ttpy)(C≡CC₁₀H₇)]PF₆, except that 3-ethynylquinoline was used to replace 1-ethynyl naphthalene. Yield: 32%. ¹H NMR (CD₃CN) δ: 2.45 (s, 3H), 7.15 (d, 2H), 7.40–8.10 (m, 10H), 8.30 (m, 2H), 8.50–8.90 (m, 6H) ppm. IR (KBr) *ν*: 2110 [w, *ν*(C≡C)] cm⁻¹. ESI-MS: *m/z* calcd for [C₃₃H₂₃N₄Pt¹⁹⁴]⁺ 669.2417, found 669.1483 (79%); calcd for [C₃₃H₂₃N₄Pt¹⁹⁵]⁺ 670.2438, found 670.1533 (100%); calcd for [C₃₃H₂₃N₄Pt¹⁹⁶]⁺ 671.2440, found 671.1492 (98%). Anal. Calcd for C₃₃H₂₃N₄PtPF₆: C, 48.58; H, 2.82; N, 6.87. Found: C, 48.18; H, 3.15; N, 6.91.

Photophysical Measurements. The electronic absorption spectra were measured on a CARY 500 dual-beam scanning UV–vis–NIR spectrophotometer. The [Pt(ttpy)(C≡CAr)]PF₆ complexes were dissolved in acetonitrile. The concentration of the solutions used

for the measurements was 1×10^{-5} mol/L. The room-temperature emission and excitation spectra were measured in acetonitrile solutions on a SPEX Fluorolog-3 fluorimeter/phosphorimeter. The low-temperature emission (77 K) spectra were measured in butyronitrile solutions (glass). The excitation wavelength was 436 nm for all samples. The solutions were purged with argon for 20 min before each measurement. The emission quantum yields of the samples were determined by the comparative method,¹⁶ in which a degassed aqueous solution of $[\text{Ru}(\text{bpy})_3]\text{Cl}_2$ ($\phi_{\text{em}} = 0.042$, excited at 436 nm)¹⁷ was used as the reference. The room-temperature emission lifetimes were determined by a time-correlated single photon counting technique on an instrument that has been previously described,¹⁸ and the low-temperature (77 K) emission lifetimes were measured on an Edinburgh LP920 laser flash photolysis spectrometer. The samples were excited by the third-harmonic output (355 nm) of a Quantel Brilliant Nd:YAG laser; the laser pulse width (fwhm) was 4.1 ns, and the repetition rate used was 1 Hz.

Transient absorption spectroscopy was carried out on an instrument described previously.¹⁹ Samples were degassed with argon for 30 min. Excitation was provided by a Nd:YAG laser (Spectra Physics GCR-14) at 355 nm. The typical pulse energy was 5 mJ/pulse, corresponding to a fluence of 20 mJ/cm² in the pump-probe region. Transient absorption decay lifetimes were determined from the multiwavelength difference-absorption data by using the SPECFIT/32 factor analysis software.²⁰

Optical Limiting Measurements. The optical limiting measurements were carried out using a Q-switched Quantel Brilliant Nd:YAG laser operated at the second-harmonic wavelength (532 nm) as the light source. The repetition rate of the laser was 10 Hz. Energies of the incident laser beam were attenuated by a combination of a half-wave plate and a polarizable cubic beam splitter. The beam was then split by a wedged beam splitter. One of the reflected beams was used to monitor the incident energy. The diameter of the transmitted beam was reduced to one-half of the original size by a telescope and was focused by a 25-cm plano-convex lens ($f/65.6$) to the center of a 2-mm sample cell. The radius of the beam waist was approximately 22.2 μm . The incident energy and the output energy were monitored by two Molelectron J4-09 pyroelectric joule meters.

Results and Discussion

Electronic Absorption Spectra. Figure 1 shows the electronic absorption spectra of platinum(II) 4'-tolylterpyridyl arylacetylide complexes in acetonitrile solutions at the concentration of 1.0×10^{-5} mol/L. The absorption obeys Beer's law when the concentration is lower than 1×10^{-4} mol/L. The absorption band maxima and the extinction coefficients are presented in Table 1. All of the spectra exhibit intense absorption bands at 260–360 nm and broad bands above 400 nm. According to previously reported spectroscopic studies,^{1–8} the UV absorption bands are due to the intraligand transitions of the terpyridyl and acetylide ligands and the charge-transfer transition involved in the Pt–C \equiv CR moieties.^{8,21} The bands above 400 nm are tentatively

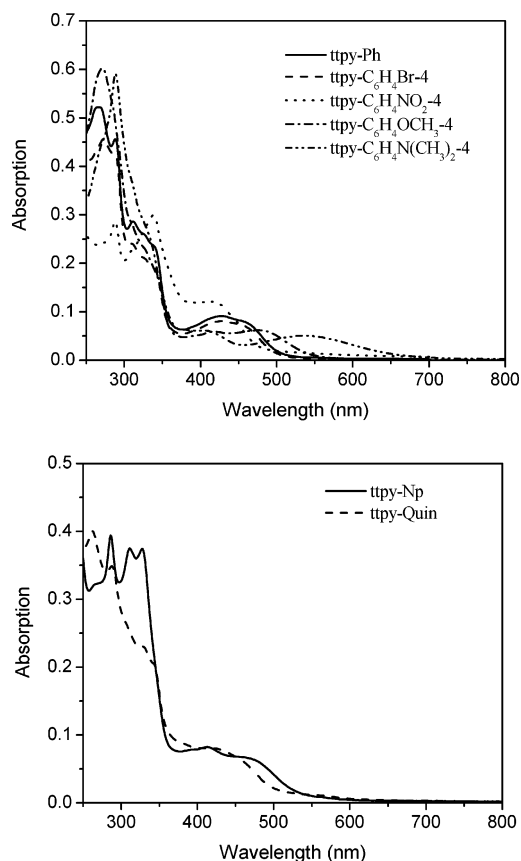


Figure 1. Electronic absorption spectra of tpy-Ar in acetonitrile solution at a concentration of 1.0×10^{-5} mol/L in a 1-cm cell.

assigned to the $d\pi(\text{Pt}) \rightarrow \pi^*(\text{tpy})$ metal-to-ligand charge-transfer (¹MLCT) transition based on the previous studies on platinum(II) terpyridyl acetylide complexes.^{6,8,22} For most of the complexes, there appears to be two distinct bands in this region, indicating that there might be two orbitally distinct MLCT transitions, e.g., $d_{xz}(\text{Pt}) \rightarrow \pi^*(\text{tpy})$ and $d_{yz}(\text{Pt}) \rightarrow \pi^*(\text{tpy})$ (assuming that the acetylide ligand is along the x axis with z perpendicular to the coordination plane), which has been suggested by Schanze and co-workers for diimine platinum(II) bis-acetylide complexes.²³

The band at ca. 420–430 nm appears to be insensitive to the para substituents on the phenylacetylide ligand, suggesting that it probably arises from the $d_{yz}(\text{Pt}) \rightarrow \pi^*(\text{tpy})$ transition, in which the d_{yz} orbital is perpendicular to the coordination plane and is unaffected by the para substituents on the phenylacetylide ligand. In contrast, the lowest-energy band above 460 nm is affected dramatically by the electron-donating ability of the ancillary substituents. Strong electron-donating groups, such as $-\text{OCH}_3$ and $-\text{N}(\text{CH}_3)_2$, cause a significant bathochromic shift of this band. This indicates that the lowest-energy band could originate from the $d_{xz}(\text{Pt}) \rightarrow \pi^*(\text{tpy})$ transition, which is sensitive to the para substituents in view of the possible resonance forms when strong electron-donating substituents are attached at the para position (Chart 2). In this view, d_{xz} is raised in energy by the

(16) Demas, J. N.; Crosby, G. A. *J. Phys. Chem.* **1971**, *75*, 991.

(17) van Houten, J.; Watts, R. J. *J. Am. Chem. Soc.* **1976**, *98*, 4853.

(18) Pinto, M. R.; Kristal, B. M.; Schanze, K. S. *Langmuir* **2003**, *19*, 6523.

(19) Wang, Y. S.; Schanze, K. S. *Chem. Phys.* **1993**, *176*, 305.

(20) Binstead, R. A. *SPECFIT/32*, version 1.0; Spectrum Software Associates: Chapel Hill, NC, 2000.

(21) Masai, H.; Sonogashira, K.; Hagihara, N. *Bull. Chem. Soc. Jpn.* **1971**, *44*, 2226.

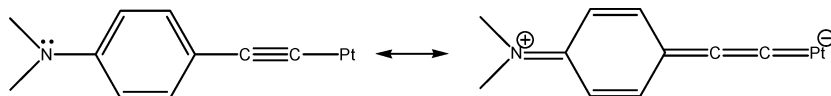
(22) Aldridge, T. K.; Stacy, E. M.; McMillin, D. R. *Inorg. Chem.* **1994**, *33*, 722.

(23) Whittle, C. Ed; Weinstein, J. A.; George, M. W.; Schanze, K. S. *Inorg. Chem.* **2001**, *40*, 4053.

Table 1. Photophysical Parameters of the Platinum(II) 4'-Tolylterpyridyl Arylacetylide Complexes

complex	$\lambda_{\text{abs}}/\text{nm}^a$ ($\epsilon/\text{dm}^3\cdot\text{mol}^{-1}\cdot\text{cm}^{-1}$)	$\lambda_{\text{em}}/\text{nm}$ (RT) ^b	$\Delta E_s/\text{cm}^{-1}$ ^c	ϕ_{em}^d	$\tau_{\text{em}}/\text{ns}$ (RT) ^e	$\tau_{\text{T}/\text{ns}}$ (RT) ^f	$\lambda_{\text{em}}/\text{nm}$ ($\tau_{\text{em}}/\mu\text{s}$) (77 K) ^g
tpty-Ph	266 (69600)	605	1820	0.0081	947	907	545 (14.52)
	289 (59700)						588 (14.18)
	312 (26800)						680 (2.00)
	430 (8000)						
	462 (9940)						
tpty-C ₆ H ₄ Br-4	273 (50300)	597	1632	0.0092	873	805	544 (15.64)
	309 (27800)						579 (13.81)
	427 (9810)						632 (2.00)
	460 (7080)						
tpty-C ₆ H ₄ NO ₂ -4	270 (27600)	552	752	0.0020	4 (10%)	76 (40%)	530 (21.49)
	288 (34400)				60 (61%)	851 (60%)	618 (1.95)
	338 (36700)				895 (29%)	700 (1.46)	
	423 (13400)						
tpty-C ₆ H ₄ OCH ₃ -4	270 (48700)	597	1431	0.0014	3 (36%)	—	550 (13.81)
	311 (25200)				43 (10%)	582 (12.91)	
	418 (4880)				817 (54%)		
	478 (5660)						
tpty-C ₆ H ₄ N(CH ₃) ₂ -4	289 (57800)	595	2241	0.0005	7 (37%)	—	525 (25.49)
	414 (3580)				112 (24%)	560 (20.83)	
	540 (4410)				936 (39%)		
tpty-Np	286 (39400)	617	1746	0.0030	23 (42%)	—	557 (20.10)
	311 (37700)				231 (39%)	594 (11.32)	
	328 (37600)				805 (19%)		
	412 (8250)						
	475 (7090)						
tpty-Quin	262 (38700)	597	1235	0.021	893	855	556 (11.90)
	288 (33120)						587
	330 (20900)						688
	343 (20000)						
	429 (8600)						

^a Linear absorption band maximum in CH₃CN solution. ^b Room-temperature emission band maximum in CH₃CN solution. ^c Thermally induced Stokes shift [$\Delta E_s = E_{00}(77\text{ K}) - E_{00}(298\text{ K})$]. ^d Room-temperature emission quantum yield in CH₃CN solution. ^e Emission decay lifetime(s) at room temperature in argon-degassed CH₃CN solution. ^f Transient absorption decay lifetime(s) in CH₃CN solution. ^g Emission band maxima and decay lifetimes at 77 K in argon-degassed butyronitrile glass.

Chart 2. Resonance Structures for tpty-C₆H₄N(CH₃)₂-4

π -donating ability of the acetylide ligand, whereas the energy of the tpty-ligand-based LUMO remains the same. Such a change reduces the energy gap between the HOMO and the LUMO, resulting in the red shift of this band.

On the other hand, the sensitivity of the lowest-energy band to the para substituents on the phenylacetylide ligand is also consistent with an acetylide-to-terpyridyl ligand-to-ligand charge-transfer (¹LLCT) transition, in which electron-donating groups increase the energy of the acetylide-ligand-based HOMO, whereas the tpty-ligand-based LUMO remains the same. For tpty-C₆H₄N(CH₃)₂-4, the LLCT transition can alternatively be viewed as occurring from the amino group to the terpyridyl ligand through the metal center,^{24,25} considering the fact that the LLCT band disappears upon protonation of the amino group (shown in Figure 2a). Therefore, it is equally probable that the lowest absorption band results either from ¹MLCT or from ¹LLCT, or even

has a mixed MLCT/LLCT character, as reported by Eisenberg and co-workers for Pt(diimine)(dithiolate) complexes.^{26,27} The possibility of the lowest-energy absorption band being due to a $\pi(\text{C}\equiv\text{CR}) \rightarrow d_{x^2-y^2}(\text{Pt})$ LMCT transition can be excluded because of the fact that no absorption band is observed above 350 nm for a platinum bis(tributylphosphine) bis(phenylacetylide) complex,²⁸ indicating that LMCT occurs at a wavelength shorter than 350 nm. The assignment of this band to an intraligand charge-transfer transition within the $-\text{C}\equiv\text{C}-\text{C}_6\text{H}_4\text{N}(\text{CH}_3)_2$ ligand can be ruled out on the basis of the fact that the intraligand transition for the compound $\text{H}-\text{C}\equiv\text{C}-\text{C}_6\text{H}_4\text{N}(\text{CH}_3)_2$ appears at a much high energy (ca. 291 nm in acetonitrile).²⁹

Figure 2 displays the electronic absorption spectra of tpty-C₆H₄N(CH₃)₂-4 and tpty-C₆H₄OCH₃-4 in CH₂Cl₂ and CH₃-

(24) Wong, K. M.-C.; Tang, W.-S.; Lu, X.-X.; Zhu, N.; Yam, V. W.-W. *Inorg. Chem.* **2005**, *44*, 1492.

(25) Yang, Q.-Z.; Wu, L.-Z.; Zhang, H.; Chen, B.; Wu, Z.-X.; Zhang, L.-P.; Tung, Z.-H. *Inorg. Chem.* **2004**, *43*, 5195.

(26) Cummings, S. D.; Eisenberg, R. *J. Am. Chem. Soc.* **1996**, *118*, 1949.

(27) Paw, W.; Lachiocotte, R. J.; Eisenberg, R. *Inorg. Chem.* **1998**, *37*, 4139.

(28) Liu, Y.; Jiang, S.; Glusac, K.; Powell, D. H.; Anderson, D. F.; Schanze, K. S. *J. Am. Chem. Soc.* **2002**, *124*, 12412.

(29) Zachariasse, K. A.; Grobys, M.; Tauer, E. *Chem. Phys. Lett.* **1997**, *274*, 372.

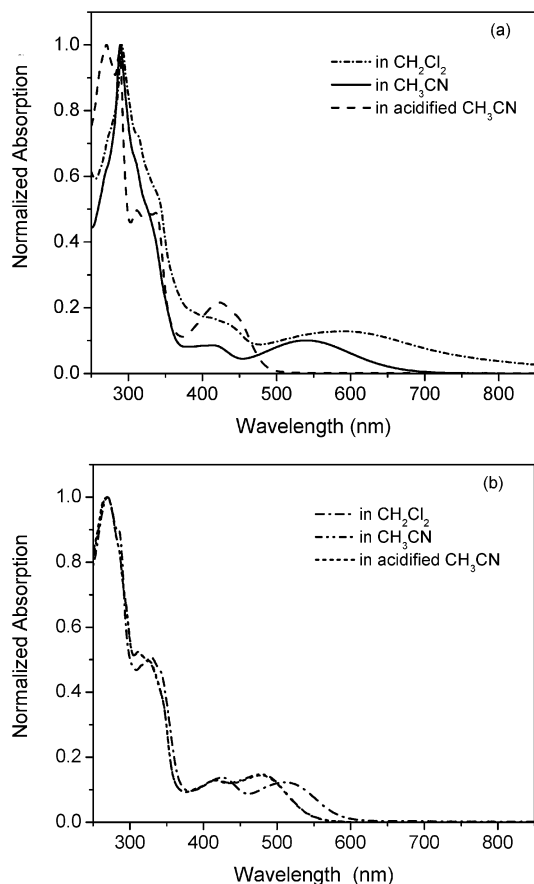


Figure 2. Normalized linear absorption spectra of (a) ttpy-C₆H₄N(CH₃)₂-4 and (b) ttpy-C₆H₄OCH₃-4 in different solvents. The spectra for ttpy-C₆H₄OCH₃-4 in acetonitrile and acidified acetonitrile overlap each other.

CN. The lowest-energy band exhibits a substantial bathochromic shift in CH₂Cl₂ in contrast to that in CH₃CN, indicating that the ground state of the complex is more polar than the excited state. Such a negative solvatochromic effect is consistent with either an MLCT or an LLCT assignment. It is also reminiscent of the Pt^{II}(diimine)(dithiolate) complexes^{26,27} and suggests a similar polar ground state in these complexes with a mixed MLCT/LLCT character. In addition, upon protonation of the -N(CH₃)₂ group by addition of dilute HCl to the acetonitrile solution, the band at 540 nm completely disappears. This suggests the involvement of the lone pair of electrons on nitrogen in the MLCT/LLCT transition. A similar solvent effect was observed for ttpy-Np, with an approximate 30-nm red shift of the lowest-energy band in CH₂Cl₂ solution.

Comparison of the charge-transfer bands of the 4'-tolylterpyridyl platinum complexes with those of the corresponding terpyridyl platinum complexes reported in the literature^{6,24} shows that they appear at almost identical positions. This indicates that the 4'-tolyl substituent on the terpyridyl ligand has a small effect on the energy level of the LUMOs [π^* (ttpy) orbital] of the complexes, which is consistent with the reported work in Pt(4'-X-ttpy)Cl⁺ systems.³ Interestingly, the molar extinction coefficients for these transitions are significantly enhanced for the 4'-tolyl-substituted complexes. This is likely due to the fact that the extended π -conjugation in the 4'-tolyl-substituted complexes

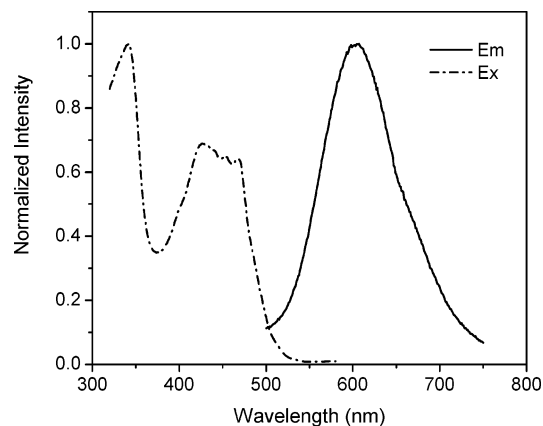


Figure 3. Excitation and emission spectra of ttpy-Ph in acetonitrile solution in a 1-cm cell. Excitation wavelength = 436 nm, concentration = 5.0×10^{-6} mol/L.

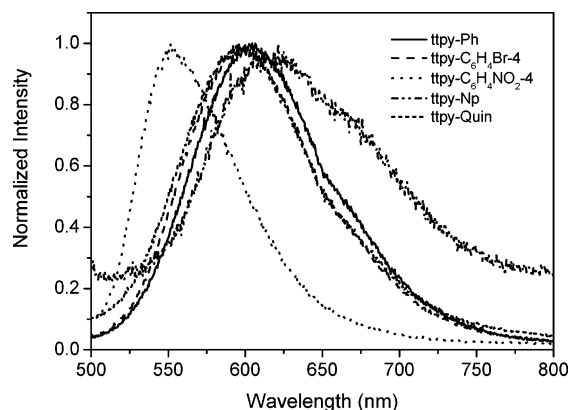


Figure 4. Normalized emission spectra of ttpy-Ar in CH₃CN solution at room temperature. Excitation wavelength = 436 nm, concentration = 8.55×10^{-6} mol/L.

increases the oscillator strength for these transitions by increasing the transition dipoles. A similar effect was observed by McMillin and co-workers in a series of phenyl-substituted Cu(I) phenanthroline complexes.³⁰

Photoluminescence. Figure 3 shows the room-temperature excitation and emission spectra for ttpy-Ph in an acetonitrile solution. The Stokes shift is approximately 4500 cm^{-1} , and the lifetime is ~ 950 ns. With reference to the previous spectroscopic studies on similar platinum(II) terpyridyl complexes, the emitting state is tentatively assigned as the ³MLCT state.^{5,6,8} The six other complexes all exhibit room-temperature emission in acetonitrile solution, as shown in Figure 4 and Table 1. Except for ttpy-C₆H₄NO₂-4, the emitting states of the other five complexes are also tentatively assigned as the ³MLCT state because of the similarities in the emission spectra to that of ttpy-Ph. However, there appears to be a lack of a systematic trend in the emission energy and lifetime. Unlike the electronic absorption spectra, the emission bands of ttpy-C₆H₄OCH₃-4 and ttpy-C₆H₄N(CH₃)₂-4 are slightly blue-shifted compared to that of ttpy-Ph. This might result from a raising of the terpyridyl π^* orbital by π back-bonding with d_{yz} because the emitting state might involve the ³ $d_{yz} - \pi^*$ state that lies in close energy proximity to ³ $d_{xz} - \pi^*$.

(30) Phifer, C. C.; McMillin, D. R. *Inorg. Chem.* **1986**, *25*, 1329.

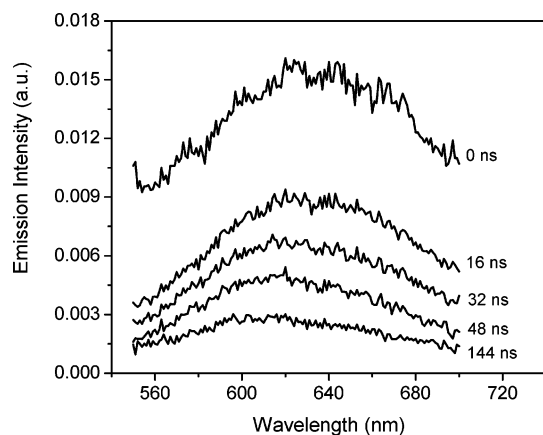


Figure 5. Time-resolved emission spectra of ttpy-Np complex in CH_3CN solution. Excitation wavelength = 355 nm.

The existence of other low-energy states in close energy proximity is further suggested by the multiexponential emission decays from the $-\text{N}(\text{CH}_3)_2-$, $-\text{OCH}_3-$, and Np-containing complexes, as shown in Table 1. From these multiexponential decays, it is clear that multiple excited states exist concomitantly, which could be $^3d_{xz}-\pi^*$, $^3d_{yz}-\pi^*$, intraligand $^3\pi-\pi^*$, and/or $^3\text{LLCT}$. These states might mix with each other, as suggested by McMillin and co-workers for platinum(II) 4'-arylterpyridyl chloride complexes,⁷ or they might not mix. In either case, multiexponential decays are possible. As suggested by Schmehl and Thummel for ruthenium(II) diimine donor/pyrene acceptor complexes, the multiexponential decays probably result from either several of these closely spaced states or luminescence from a single state with the fast component reflecting the preequilibrium relaxation of the emitting state and the longer decay processes involving relaxation of the equilibrated states.³¹

The presence of closely spaced excited states could also be accountable for the low emission quantum yields for ttpy- $\text{C}_6\text{H}_4\text{OCH}_3$ -4 and ttpy- $\text{C}_6\text{H}_4\text{N}(\text{CH}_3)_2$ -4. As was proposed previously for the donor-acceptor-substituted complex $[(\text{bpy})\text{Re}^{\text{I}}(\text{CO})_3\text{DMABA}]^+$ (DMABA = dimethylaminobenzonitrile), MLCT emission can be strongly quenched via the efficient LLCT radiationless decay pathway in polar solvents because of the significantly increased MLCT \rightarrow LLCT interconversion rate.^{32,33}

Figure 5 displays the time-resolved emission spectra for ttpy-Np. It is clear that the decay rates vary at different wavelengths. Although such wavelength dependence is also consistent with impurities, this assignment for the multiexponential behavior is not favored because similar emission spectra are obtained when the complex is excited at different excitation wavelengths and the excitation spectra monitored at different emission wavelengths remain the same. This suggests that no emissive impurities are present in the solution.

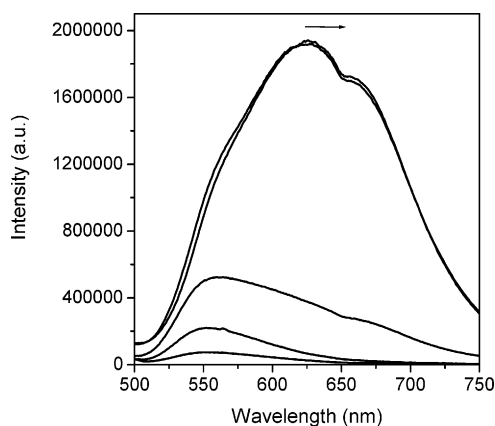


Figure 6. Concentration-dependent emission spectra of ttpy- $\text{C}_6\text{H}_4\text{NO}_2$ -4 in acetonitrile solution at room temperature ($\lambda_{\text{ex}} = 436$ nm). In order of increasing intensity, the concentrations are: 5.2×10^{-6} , 1.1×10^{-5} , 3.0×10^{-5} , 5.3×10^{-5} , and 1.6×10^{-4} mol/L.

For ttpy- $\text{C}_6\text{H}_4\text{NO}_2$ -4, as will be discussed later, the emission probably emanates from the $^3\pi,\pi^*$ state localized at the nitrophenylacetylide ligand. The multiexponential decays for this complex are likely due to excimer formation at relatively low concentration ($\sim 5 \times 10^{-5}$ mol/L), which is demonstrated by the concentration dependence study of the emission spectra. As shown in Figure 6, the emission band exhibits a substantial red shift when the concentration is increased, changing from ca. 553 nm at a concentration of 5.2×10^{-6} mol/L to ca. 626 nm when the concentration of the solution is increased to 5.3×10^{-5} mol/L.

In contrast to ttpy- $\text{C}_6\text{H}_4\text{NO}_2$ -4, no excimer emission was observed from the rest of the complexes, even at the very high concentration of ca. 10^{-3} mol/L. For example, for ttpy-Quin, the emission band maximum in CH_3CN solution remains the same as the concentration is increased from 10^{-7} to 10^{-3} mol/L. However, the intensity of the emission increases with concentration for $c \leq 1.03 \times 10^{-4}$ mol/L, and then at higher concentration, it decreases with increasing concentration, presumably as a result of self-quenching. A similar result was obtained for solutions of ttpy-Ph. The notion of the decreased emission intensity at higher concentrations being due to self-quenching is confirmed by emission lifetime measurements. For example, the lifetime for ttpy-Ph is 780 ns at $c = 1 \times 10^{-5}$ mol/L, 740 ns at $c = 5 \times 10^{-5}$ mol/L, and 476 ns at $c = 5 \times 10^{-4}$ mol/L, and the lifetime decreases to 397 ns when the concentration is increased to 1×10^{-3} mol/L. The self-quenching constant obtained from the slope of the k_{obs} versus complex concentration plot is $1.3 \times 10^9 \text{ M}^{-1} \text{ s}^{-1}$. For ttpy- $\text{C}_6\text{H}_4\text{OCH}_3$ -4/ CH_3CN and ttpy- $\text{C}_6\text{H}_4\text{N}(\text{CH}_3)_2$ -4/ CH_3CN solutions, the self-quenching occurs at concentrations greater than 1.3×10^{-5} mol/L. Self-quenching has also been observed in the mono platinum(II) complexes of 6-phenyl-2,2'-bipyridine by Che and co-workers³⁴ and in (diimine) $\text{Pt}(-\text{C}\equiv\text{C}-\text{Ar})_2$ complexes by Eisenberg and co-workers.¹³ The bimolecular self-quenching rate constants were reported to be on the order of $10^9 \text{ M}^{-1} \text{ s}^{-1}$.^{13,34}

(31) Simon, J. A.; Curry, S. L.; Schmehl, R. H.; Schatz, T. R.; Piotrowiak, P.; Jin, X.; Thummel, R. P. *J. Am. Chem. Soc.* **1997**, *119*, 11012.

(32) Perkins, T. A.; Pourreau, D. B.; Netzel, T. L.; Schanze, K. *J. Phys. Chem.* **1989**, *93*, 4511.

(33) Perkins, T. A.; Humer, W.; Netzel, T. L.; Schanze, K. *J. Phys. Chem.* **1990**, *94*, 2229.

(34) Lai, S.-W.; Chan, M. C.-W.; Cheung, T.-C.; Peng, S.-M.; Che, C.-M. *Inorg. Chem.* **1999**, *38*, 4046.

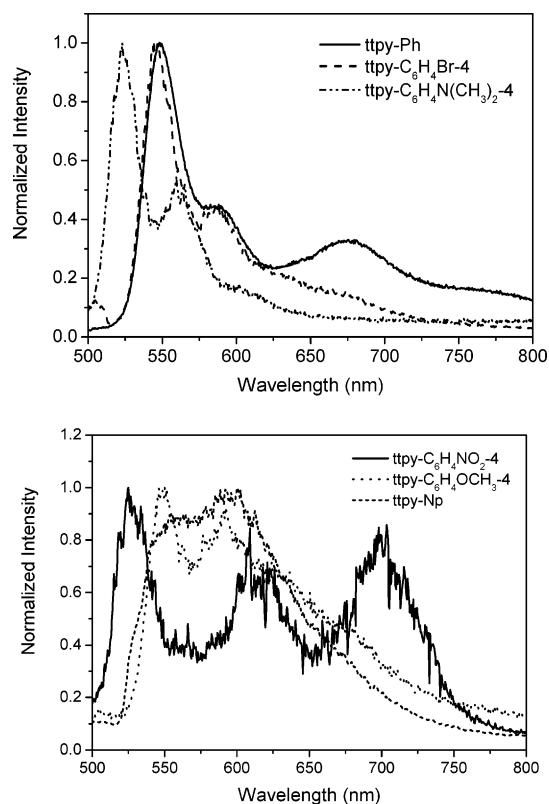


Figure 7. Emission spectra of tpy-Ar in butyronitrile solution (glass) at 77 K. Excitation wavelength = 436 nm, concentration $\approx 10^{-4}$ mol/L.

It is noteworthy that, in contrast to the very small influence of the 4'-tolyl substituent on the electronic absorption spectra, there appears to be a pronounced effect in emission upon introduction of the 4'-tolyl substituent on the terpyridyl ligand. For example, the tpy-C₆H₄OCH₃-4 and tpy-C₆H₄N(CH₃)₂-4 complexes exhibit detectable emission in solution, whereas the corresponding terpyridyl complexes without the 4'-tolyl substituent do not.^{6,24}

The luminescence spectra of these complexes in butyronitrile at 77 K are presented in Figure 7. At 77 K, the emission bands shift to higher energy and exhibit a clear vibronic structure. For tpy-Ph, the major band appears at ca. 545 nm with a shoulder near 588 nm. This is consistent with the previous spectroscopic studies on similar platinum(II) terpyridyl complexes.^{5,6,8} The spacing of the vibronic progression (~ 1340 cm⁻¹) corresponds to the aromatic vibrational mode of the terpyridyl ligand.⁶ Because the rigidochromic shift (i.e., large thermally induced Stokes shift $\Delta E_s \approx 1820$ cm⁻¹) is a characteristic of the charge-transfer emission, we attribute the emitting state at 77 K as the ³MLCT state. The ³MLCT assignment for low-temperature emission has been suggested by Eisenberg and co-workers for diimine bis(acetylide) complexes.¹³ This assignment also applies to the other complexes except for tpy-C₆H₄NO₂-4. For tpy-C₆H₄NO₂-4, the lack of a significant thermally induced Stokes shift ($\Delta E_s \approx 752$ cm⁻¹) indicates that the 77 K emission does not originate from an MLCT manifold. Rather, it probably arises from an intraligand ³ π, π^* state that involves the nitrophenylacetylide ligand, as proposed by Schanze and co-workers for the diimine platinum bis-4'-nitrophenylacetylide complex.²³ The two low-energy emission bands observed in the

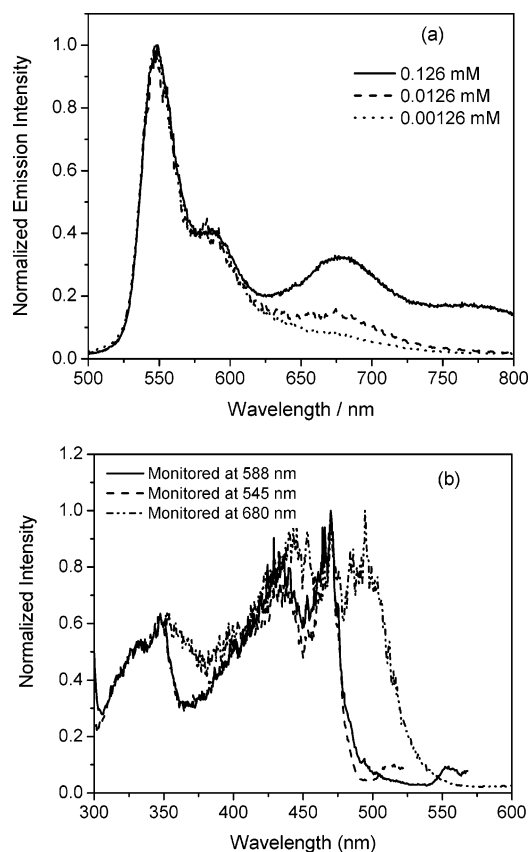


Figure 8. (a) Concentration-dependent emission spectra of tpy-Ph-Cl in methanol/ethanol glass at 77 K. Excitation wavelength = 436 nm. (b) Excitation spectra of 1.26×10^{-4} mol/L methanol/ethanol glass of tpy-Ph-Cl monitored at different emission wavelengths.

tpy-C₆H₄NO₂-4 complex but not in the diimine platinum bis-4'-nitrophenylacetylide complex are due to the formation of ground-state aggregates at the concentration used for the measurement, as discussed further below.

The low-energy peaks at ca. 680 nm for tpy-Ph, 618 and 700 nm for tpy-C₆H₄NO₂-4, and 688 nm for tpy-Quin exhibit a concentration dependence, as exemplified by tpy-Ph in Figure 8a. This feature suggests that an excimer or ground-state complex is responsible for these low-energy bands. Che and co-workers ascribed the structureless low-energy band at high concentration at 77 K for platinum(II) 2,6-diphenylpyridine complexes to the formation of ³ π, π^* excimer.³⁵ However, this assignment does not apply to the aforementioned complexes. A study of the excitation spectra of tpy-Ph, tpy-C₆H₄NO₂-4, and tpy-Quin at different emission wavelengths shows that the excitation spectrum monitored at the low-energy band is different from those monitored at the high-energy structured bands, as exemplified in Figure 8b for the tpy-Ph complex. With reference to the work reported by Yam and co-workers for the platinum(II) 2,6-biphenylpyridyl complexes,³⁶ the broad low-energy band(s) at 77 K originate(s) from an emissive state resulting from ground-state aggregation of the complexes. The appearance

(35) Lu, W.; Chan, M. C.; Cheung, K.-K.; Che, C.-M. *Organometallics* **2001**, *20*, 2477.

(36) Yam, V. W.-W.; Tang, R. P.-L.; Wong, K. M.-C.; Lu, X.-X.; Cheung, K.-K.; Zhu, N. *Chem. Eur. J.* **2002**, *8*, 4066.

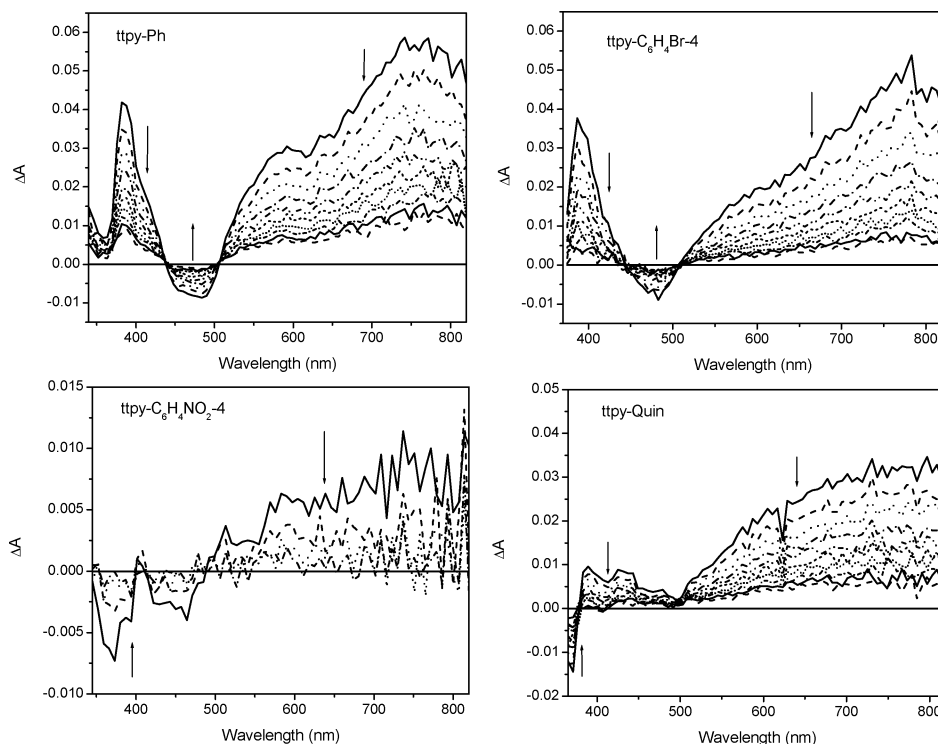


Figure 9. Transient absorption difference spectra of ttpy-Ar in argon-degassed acetonitrile solution at room temperature following 355-nm excitation. The time increments are 160 ns for ttpy-Ph, ttpy-C₆H₄Br-4, and ttpy-Quin and 40 ns for ttpy-C₆H₄NO₂-4 beginning immediately after the laser pulse. Arrows indicate the direction of change of ΔA with increasing time.

of the low-energy emission band(s) at 77 K for glasses but not at room temperature for solutions at similar concentrations indicates that the association constant for the aggregation process could be too small to be observed at room temperature. This hypothesis was further supported by the electronic absorption spectra measurement at different concentrations. No bathochromic shift or peak broadening was observed for ttpy-Ph from the concentration of 10^{-6} to 10^{-4} mol/L. Unfortunately, the measurement of the concentration-dependent electronic absorption spectra at 77 K could not be carried out because of our current instrument limitations.

Transient Absorption (TA) Spectroscopy. The time-resolved transient difference absorption spectra are illustrated in Figure 9 for complexes ttpy-Ph, ttpy-C₆H₄Br-4, ttpy-C₆H₄NO₂-4, and ttpy-Quin. Transient absorption from complexes ttpy-C₆H₄OCH₃-4, ttpy-C₆H₄N(CH₃)₂-4, and ttpy-Np was too weak to be observed. The TA spectra of ttpy-Ph and ttpy-C₆H₄Br-4 are similar, with each spectrum featuring a moderately intense, narrow absorption band in the near-UV region ($\lambda_{\text{max}} \approx 390$ nm); a bleaching band from 430 to 500 nm; and a broad, strong absorption throughout the visible region and extending into the near-IR region. The bleaching band occurs in the region corresponding to the MLCT transition, and this feature is consistent with the excited state having MLCT character. In addition, τ_{TA} coincides with τ_{em} , indicating that the transient absorption arises from the same excited state that is responsible for the emission, i.e., from a state that exhibits ³MLCT character. Alternatively, the absorbing transient might be in equilibrium with the emitting excited state. The transient absorption in the visible to near-IR region likely results from the terpyridyl anion radical that

is present in the MLCT state, which is in line with the TA absorptions of diimine platinum(II) bis-acetylide complexes.²³ The MLCT assignment is further supported by the fact that the shapes of these TA spectra are very similar to those of the ruthenium dinuclear complexes (tp)₂Ru(tpy-tpy)Ru(tp)⁴⁺ and (tp)₂Ru(tpy-ph-tpy)Ru(tp)⁴⁺, which are known to have lowest excited states based on the metal-to-bridged ligand charge-transfer transition.³⁷ For ttpy-Quin, the bleaching band is not as obvious as those for ttpy-Ph and ttpy-C₆H₄Br-4. Nevertheless, the appearance of a moderately intense, broad absorption band in the visible to near-IR region and the coincidence of τ_{TA} with τ_{em} suggest that the transients might also represent the ³MLCT excited-state complex. On the other hand, the similarity of the shape of the spectrum in the visible to near-IR region to that of the diimine platinum bis-4'-nitrophenylacetylide complex (complex 2b)²³ and the appearance of the bleaching band in the UV region also indicate that the excited state involves the acetylide ligands, i.e., the lowest excited state for TA absorption involves a ³ π, π^* state that is localized on the quinoliny acetylide ligand. This is particularly true for the ttpy-C₆H₄NO₂-4 complex, in which even the emitting state is dominated by the ³ π, π^* state localized on the nitrophenylacetylide ligand as described earlier.

Optical Limiting of Nanosecond Laser Pulses. It is well-known that reverse saturable absorption can lead to optical limiting, which reduces the transmittance when the laser intensity is higher than the limiting threshold. One criterion

(37) Hammarström, L.; Barigelletti, F.; Flamigni, L.; Indelli, M. T.; Armaroli, N.; Calogero, G.; Guardigli, M.; Sour, A.; Collin, J.-P.; Sauvage, J.-P. *J. Phys. Chem. A* **1997**, *101*, 9061.

for reverse saturable absorption to occur is that the excited-state absorption cross section must exceed the ground-state absorption cross section. The higher the ratio of the cross section of the excited-state absorption to that of the ground-state absorption, the stronger the reverse saturable absorption. To increase this ratio, one can either decrease the ground-state absorption or increase the excited-state absorption. In addition, optical limiting of nanosecond laser pulses is generally dominated by the triplet excited-state absorption when the intersystem crossing time is shorter than the laser pulse width. It has been reported that the intersystem crossing time for a platinum ethynyl complex is ~ 330 ps.³⁸ It is reasonable to assume that the intersystem crossing rate is also rapid for platinum(II) terpyridyl complexes. This hypothesis is supported by the fact that the emission of platinum(II) terpyridyl complexes originates from the triplet excited state, as discussed in the Photoluminescence section. Thus, the optical limiting of nanosecond laser pulses by platinum(II) terpyridyl complexes should be dominated by the triplet excited-state absorption. In this case, a long lifetime, high quantum yield, and large absorption cross section for the triplet excited state would be expected to enhance the optical limiting of nanosecond laser pulses.

As shown in Figure 1, the absorption spectra of the complexes studied exhibit weak or no ground-state absorption above 500 nm, whereas the transient difference absorption spectra of ttpy-Ph, ttpy-C₆H₄Br-4, and ttpy-Quin, shown in Figure 9, exhibit a broad and moderately intense absorption band in this spectral region. This indicates that reverse saturable absorption could occur throughout the visible to near-IR region. In addition, as discussed earlier in the Photoluminescence section and shown in Table 1, the triplet excited-state lifetimes of ttpy-Ph, ttpy-C₆H₄Br-4, and ttpy-Quin complexes are quite long. The quantum yields of the triplet excited states were measured by laser-induced optoacoustic spectroscopy (LIOAS) as described previously³⁹ and were found to be $88 \pm 7\%$ for ttpy-Ph, $77 \pm 8\%$ for ttpy-C₆H₄Br-4, and $60 \pm 5\%$ for ttpy-Quin. Such high quantum yields are the result of the heavy-metal-enhanced spin-orbital coupling effect. These characteristics combined with the broadband reverse saturable absorption suggest that these complexes are promising candidates for broadband optical limiting applications.

To demonstrate this possibility, a study of the optical limiting of ttpy-Ph, ttpy-C₆H₄Br-4, and ttpy-Quin for 4.1-ns laser pulses was conducted, and the results are shown in Figure 10. It is obvious that the curves for these samples deviate significantly from the linear absorption line, suggesting the occurrence of optical limiting. The limiting threshold at $T/T_0 = 0.9$ and the nonlinear transmittance at incident fluence of 2.5 J/cm² are listed in Table 2. As can be seen from Figure 10 and Table 2, the optical limiting performances of these complexes are influenced dramatically by the nature of the chemical structures. ttpy-Ph yields the strongest optical limiting, with transmittance dropping to 28%

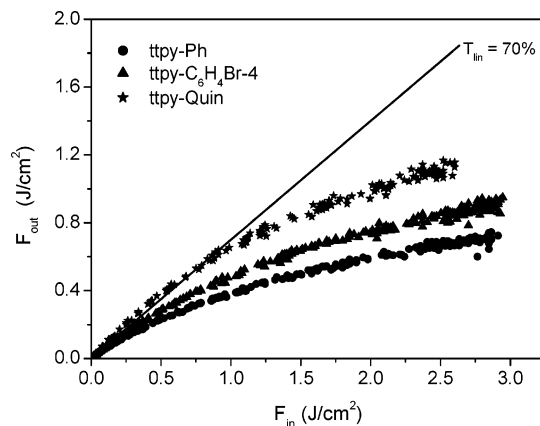


Figure 10. Optical limiting of platinum(II) 4'-tolylterpyridyl arylacetylde complexes in acetonitrile in a 2-mm cell. The linear transmission for each of the solutions is 70%.

Table 2. Optical Limiting Parameters of the Platinum(II) 4'-Tolylterpyridyl Arylacetylde Complexes in Acetonitrile Solution

complex	σ_0^a (cm ²)	F_{th}^b (J/cm ²) (at $T/T_0 = 0.9$)	T_{lim}^c	σ_{eff}/σ_g
ttpy-Ph	2.43×10^{-19}	0.048	0.28	>3.57
ttpy-C ₆ H ₄ Br-4	7.18×10^{-19}	0.144	0.34	>3.02
ttpy-Quin	1.12×10^{-18}	1.09	0.44	>2.30

^a Ground-state absorption cross section at 532 nm. ^b Optical limiting threshold when the transmittance drops to 90% of the linear transmittance. ^c Nonlinear transmittance at incident fluence of 2.5 J/cm².

at the incident fluence of 2.5 J/cm². The strength of the optical limiting appears to be in the order ttpy-Ph > ttpy-C₆H₄Br-4 > ttpy-Quin. The stronger optical limiting of ttpy-Ph can be attributed to its higher triplet excited-state quantum yield.

To quantitatively compare the strength of optical limiting abilities of these complexes, the figure of merit σ_{eff}/σ_g is used, where σ_{eff} is the effective excited-state absorption cross section and σ_g is the ground-state absorption cross section. At the incident fluence of 2.5 J/cm², which is much higher than the saturable fluence defined as $F_{sat} = hv/\sigma_g\Phi_t$,⁴⁰ the ground state is greatly bleached, and the excited-state population is mainly distributed at the triplet state. In this case, σ_{eff}/σ_g can be defined as $\sigma_{eff}/\sigma_g = (\ln T_{sat})/(\ln T_{lin})$,⁴⁰ where T_{sat} is the transmittance at the saturable fluence and T_{lin} is the linear transmittance. However, the damage threshold of the quartz cell (5 J/cm²) limited the maximum incident fluence that could be used in our experiments; therefore, we were unable to reach the saturable transmittance. Nevertheless, the lowest transmittance at the highest incident fluence can be used to calculate a lower bound to σ_{eff}/σ_g for these complexes. The results are listed in Table 2.

In addition to the excellent optical limiting performance, these three complexes show exceptional thermal and photochemical stability in the solid and in CH₃CN solution. After 2 years of storage in air and exposure to UV and visible laser light radiations, the complexes remain unchanged.

(38) McKay, T. J.; Bolger, J. A.; Staromlynska, J.; Davy, J. R. *J. Chem. Phys.* **1998**, *108*, 5537.

(39) Walters, K. A.; Schanze, K. S. *Spectrum* **1998**, *11* (2), 1.

(40) Perry, J. W.; Mansour, K.; Marder, S. R.; Perry, K. J.; Alvarez, D. Jr.; Choong, I. *Opt. Lett.* **1994**, *19*, 625.

Conclusions

Platinum(II) 4'-tolylterpyridyl arylacetylide complexes exhibit a low-energy solvatochromic charge-transfer transition ($^1\text{MLCT}$ or/and $^1\text{LLCT}$) in their electronic absorption spectra that is sensitive to the para substituents on the phenylacetylide ligand. Except for $\text{tpty-C}_6\text{H}_4\text{NO}_2\text{-4}$, which likely emits from an $\text{IL } ^3\pi,\pi^*$ state involving the nitrophenylacetylide ligand, the emission of the other complexes emanates from the $^3\text{MLCT}$ state. Complexes containing electron-rich arylacetylide ligands, i.e., $\text{tpty-C}_6\text{H}_4\text{OCH}_3\text{-4}$, $\text{tpty-C}_6\text{H}_4\text{N(CH}_3)_2\text{-4}$, and tpty-Np , exhibit multiexponential emission decays due to the presence of multiple low-energy states in close energy proximity. The transient absorption difference spectra of tpty-Ph , $\text{tpty-C}_6\text{H}_4\text{Br-4}$, $\text{tpty-C}_6\text{H}_4\text{NO}_2\text{-4}$, and tpty-Quin exhibit moderately intense, broad absorption bands in the visible region and extending into the near-IR region that might originate from the same excited state that emits or from a state that is in equilibrium with the emitting state. The complexes with electron-rich arylacetylide ligands

exhibit no transient absorption. Moreover, because of the high quantum yield and the relatively long lifetime of the triplet excited state, as well as the broad, moderately intense triplet excited-state absorption in the visible spectral range, tpty-Ph , $\text{tpty-C}_6\text{H}_4\text{Br-4}$, and tpty-Quin have been demonstrated to exhibit significant optical limiting for nanosecond laser pulses at 532 nm. They are promising candidates for broadband optical limiting of nanosecond laser pulses.

Acknowledgment is made to the Donors of the American Chemical Society Petroleum Research Fund for support of this research. W.S. also acknowledges the North Dakota EPSCoR for support (EPSCoR Seed Award, Instrumental Award, and Faculty Start-up Award). K.S. and Y.L. acknowledge the National Science Foundation for support of their work (CHE- 0211252). We also thank the editor and the anonymous reviewers for valuable comments and suggestions.

IC049266N